



Published in final edited form as:

Invest Radiol. 2016 December ; 51(12): 786–796. doi:10.1097/RLI.0000000000000279.

A proposed CT contrast agent using carboxybetaine zwitterionic tantalum oxide nanoparticles: Imaging, biological, and physicochemical performance

Paul F. FitzGerald, AAS*, Matthew D. Butts, PhD*, Jeannette C. Roberts, MS*, Robert E. Colborn, PhD*, Andrew S. Torres, PhD*, Brian D. Lee, PhD MBA DABT*, Benjamin M. Yeh, MD†, and Peter J. Bonitatibus Jr., PhD*,‡

*GE Global Research Center, Niskayuna, NY

†University of California, San Francisco, San Francisco, CA

Abstract

Objectives—To produce and evaluate a proposed computed tomography (CT) contrast agent based on carboxybetaine zwitterionic (CZ) coated soluble tantalum oxide nanoparticles (CZ-TaO NPs). We chose tantalum to provide superior imaging performance compared to current iodine-based clinical CT contrast agents. We developed the CZ coating to provide biological and physical performance similar to that of current iodinated contrast agents. The aim of this study was to evaluate the imaging, biological, and physicochemical performance of this proposed contrast agent compared to clinically-used iodinated agents.

Materials and Methods—We evaluated CT imaging performance of our CZ-TaO NPs compared to an iodinated agent in live rats, imaged centrally-located within a tissue-equivalent plastic phantom that simulated a large patient. To evaluate vascular contrast enhancement, we scanned the rats' great vessels at high temporal resolution during and following contrast agent injection. We performed several *in vivo* CZ-TaO NP studies in healthy rats to evaluate tolerability. These studies included injecting the agent at the anticipated clinical dose (ACD) and at 3 times and 6 times the ACD, followed by longitudinal hematology to assess impact to blood cells and organ function (from 4 hours to 1 week). Kidney histological analysis was performed 48 hours after injection at 3 times the ACD. We measured the elimination half-life of CZ-TaO NPs from blood, and we monitored acute kidney injury biomarkers with a kidney injury assay using urine collected from 4 hours to 1 week. We measured tantalum retention in individual organs and in the

†Corresponding Author: *Peter J. Bonitatibus, Jr., PhD*, One Research Circle, Niskayuna, NY 12309, bonitati@ge.com, Phone: (518) 387 6888, Fax: (518) 387 7548.

The authors declare no conflicts of interest.

List of Supplemental Digital Content

- Supplemental Digital Content 1: Figures: Structures and sizes of iodixanol and iopromide
- Supplemental Digital Content 2: Text: Vessel segmentation and contrast enhancement quantification
- Supplemental Digital Content 3: Text: Detailed synthesis and characterization
- Supplemental Digital Content 4: Video: Example of vessel tracking and segmentation process
- Supplemental Digital Content 5: Figures: Attenuation curve signal processing
- Supplemental Digital Content 6: Tables: Complete blood count (CBC) and clinical chemistry
- Supplemental Digital Content 7: Figures: Complete blood count (CBC)
- Supplemental Digital Content 8: Figure: Blood half-life
- Supplemental Digital Content 9: Figure: Kidney toxicity study: MSD assay

whole carcass 48 hours after injection at ACD. CZ-TaO NPs were synthesized and analyzed in detail. We used multi-dimensional nuclear magnetic resonance (NMR) to determine surface functionality of the nanoparticles. We measured nanoparticle size and solution properties (osmolality and viscosity) of the agent over a range of tantalum concentrations, including the high concentrations required for standard clinical CT imaging.

Results—CT imaging studies demonstrated image contrast improvement of approximately 40–50% using CZ-TaO NPs compared with an iodinated agent injected at the same mass concentration. Blood and organ analyses showed no adverse effects following injection in healthy naïve rats at 3 times the ACD. Retention of tantalum at 48 hours after injection was less than 2% of the injected dose in the whole carcass, which very closely matched the reported retention of existing commercial iodine-based contrast agents. Urine analysis of sensitive markers for acute kidney injury showed no responses at 1 week following injection at 3 times the ACD; however, a moderate response in the neutrophil gelatinase-associated lipocalin (NGAL) biomarker was measured at 24 and 48 hours. Compared to other tantalum oxide nanoparticles reported in the literature, CZ-TaO NPs had relatively low osmolality and viscosity at concentrations >200 mg Ta/mL, and were similar in these physical properties to dimeric iodine-based contrast agents.

Conclusions—We found that a CZ-TaO NP-based contrast agent is potentially viable for general-purpose clinical CT imaging. Our results suggest that such an agent can be formulated with clinically-viable physicochemical properties, can be biologically safe and cleared rapidly in urine, and can provide substantially improved image contrast at CT compared to current iodinated agents.

Keywords

contrast agent; nanoparticle; computed tomography; CT; imaging; tantalum oxide; zwitterions

Introduction

Iodine-based molecular contrast agents represent a historically well-tolerated class of pharmaceuticals for X-ray and CT imaging, especially in patients with normal kidney function. At present, clinicians can select from either monomeric tri-iodinated aromatic compounds (examples: iohexol and iopromide) or dimeric versions of these agents (examples: iodixanol and iotrolan). Both classes of these agents offer individual advantages at formulated concentration (240–370 mg I/mL): monomeric agents have relatively low viscosity compared to dimeric agents, and dimeric agents are hypo-osmolar, allowing for the addition of excipients to make clinical products iso-osmolar with blood plasma. An important drawback of iodinated agents is their reduced X-ray attenuation when imaged with higher energy X-ray spectra, as are commonly used for obese patients.

There is a need for more effective contrast agents that would permit imaging with lower radiation dose than is possible today, as well as improved imaging of large-to-obese patients. Although there is currently some debate over the prevalence of contrast-induced nephropathy (CIN),¹ new agents may be needed to better moderate the effects of iodinated contrast agents on patients with compromised kidney function or who have experienced an allergic reaction to iodinated agents.² Attempts to develop a new clinical imaging agent that

could be formulated to feature both iso-osmolality with blood (~290 mOsm/kg) and low viscosity (~4–6 mPa.s) have not yielded a clinically viable product. This anticipated product would provide several advantages over current contrast agents. Iso-osmolar agents have been shown to prevent some acute effects of hyperosmolar agents (heat sensation, pain, cardiac hemodynamics).^{3–5} Additionally, lower viscosity agents require lower injection pressures and are significantly more efficient in their clearance from the kidneys, which could potentially improve overall renal safety.^{3,6} An ideal contrast agent would satisfy both of these criteria and enable improved image quality or reduced radiation dose compared with current iodine-based agents.

Heavy metal nanoparticles offer a potential clinical solution to this challenge, provided they can be synthesized at reasonable cost and prove to be well-tolerated and safe.^{7–10} Several years ago, a new class of tantalum oxide (TaO) nanoparticles (NPs) was reported that showed promise as CT imaging agents.^{11–15} These zwitterionic particles are less than 10 nm in diameter and comprise organofunctional silane-based shells to stabilize and protect the TaO cores. Zwitterionic shells result in particles that are charge neutral as a whole, but have distributed positive and negative charge over the surface of the particle. Because the charges are covalently bound to each other, contrast agents containing zwitterionic nanoparticles are considered non-ionic. We have found that the specific design of the zwitterionic ligand can affect the osmolality, viscosity, and renal clearance of the nanoparticles; we hypothesized that a design could be found that allows the nanoparticle to satisfy all physicochemical and biological safety requirements. Furthermore, a recent report¹⁶ suggests that tantalum is the most promising candidate among the chemical elements evaluated for use in general-purpose CT contrast agents in terms of toxicity, cost, and availability. In addition, other work¹⁷ predicts up to 65% improvement in CT image contrast for large-to-obese patients when tantalum-based rather than iodinated contrast agents are given at equal mass concentration. Tantalum could provide improved CT image quality, reduced contrast agent dose, reduced radiation dose, or a combination of the three benefits.

With conventional small-molecule iodinated agents, CT contrast enhancement within the arterial lumen is on the order of a few hundred HU. This suggests iodine concentration on the order of 10 mg iodine/mL blood¹⁶ (after dilution by the blood from the intravenously-injected concentration of 240–370 mg/mL). The size of the molecules in these iodinated agents is approximately 1.3 nm for monomeric molecules and approximately 2.2 nm for dimeric molecules. Figures in Supplemental Digital Content 1, show the structure and size of typical iodinated molecules, as estimated by ChemBioDraw® (PerkinElmer Informatics, Waltham, MA).

Detailed discussion of vascular endothelial permeability is beyond the scope of this work; however, a brief review of the feature sizes involved can shed light on the nanoparticle size that would allow for rapid equilibrium across the endothelium as seen with small-molecule iodinated agents. Capillary permeability is influenced by many factors, pore size among them.

When contrast agent-containing blood enters the capillary beds of coronary, pulmonary, splanchnic, and skeletal muscle tissue, small-diameter “extracellular, extravascular” contrast

agents begin to redistribute into the interstitial space. The capillary endothelium readily permits passage of molecules of approximately 3–4 nm through interendothelial junctions (IEJs).¹⁸ Therefore, we hypothesize that in these tissues, nanoparticles with a narrow distribution centered at 3 nm could behave similarly to the approximately 1–2 nm iodinated molecules via IEJ transport.

The porosity of capillaries in other organ parenchyma differs greatly from that already discussed. In the fenestrated capillaries found in certain organs, small molecules or nanoparticles can readily leave the vasculature, because the endothelial fenestra size is 60–70 nm in endocrine tissue, gastrointestinal mucosa, and renal peritubular capillaries, and 100 nm or larger in the discontinuous capillaries of the spleen, bone marrow, and in liver sinusoidal endothelial cells.¹⁹ In organs containing either of those capillary types, substantial interstitial contrast enhancement of the organ parenchyma occurs rapidly with conventional iodinated agents. This enhancement is more persistent than the primary arterial bolus, and results in contrast enhancement of tens of HU in the liver (implying concentration of a few mg iodine/mL tissue) to many hundreds of HU in the kidney (corresponding to greater than 10 mg iodine/mL tissue) in the venous phase and nephrographic phases of enhancement. Similarly, endothelial permeability is increased in many diseased states such as inflammation or neoplasm, which frequently show relatively rapid equilibration of extracellular, extravascular contrast agents between the vascular lumen and interstitial space at imaging.

We believe that based on the above considerations, a contrast agent with a particle size of a few nanometers could show similar pharmacokinetic distribution as conventional iodinated agents, both in tissues with continuous and with fenestrated capillaries. Therefore, we hypothesize that such an agent could be used as a general-purpose contrast agent, if biological safety and physicochemical requirements are satisfied.

The published results^{11–15} suggest that TaO NP agents can be formulated at concentrations required for CT imaging, are well-tolerated at high dose, and are eliminated rapidly via renal clearance mechanisms with low tissue retention in injected rats. However, the first reported zwitterionic compound¹³ did not meet physicochemical criteria that are required for clinical use: iso-osmolality with blood, low viscosity, and tissue retention in injected rats lower than or equal to that reported for iodine-based contrast agents.^{20,21} The CZ-TaO NP-based agent reported herein is a new variation of a zwitterionic-coated TaO NP (Figure 1) and represents significant progress toward imparting nanoparticles with physical and biological properties as favorable as a dimeric iodine-based contrast agent that is routinely used clinically. Furthermore, our report provides the first *in vivo* imaging evidence of the substantially higher CT image contrast enhancement provided by a practical contrast agent containing a high atomic number (high Z) element compared to a conventional iodinated agent at the same mass concentration.

Materials and Methods

All animal experiments were performed in accordance with protocols approved by the Institutional Animal Care and Use Committee (IACUC) at our institution.

Imaging Studies

Contrast agent preparation—We prepared our proposed CZ-TaO NP agent by formulating to iso-osmolality using 10X concentrated phosphate-buffered saline (PBS), which resulted in a nominal mass concentration of 138 mg Ta/mL. We similarly diluted clinically-used iodinated agent (iopromide) to the same nominal mass concentration, 138 mg I/mL (see Table 1). We measured the actual active element concentration in the formulated agents using inductively coupled plasma optical emission spectroscopy (ICP-OES) quantification (Spectro Arcos, Kleve Germany).

Hybrid model of a coronary CT angiography (CCTA) in a large patient—To represent a clinical CCTA exam of a large patient, we constructed a phantom (Figure 2) containing a live rat within a water-equivalent plastic phantom. We used male Lewis rats (Charles River, Wilmington MA), procured at approximately 325–340 g and grown in our facility to approximately 340–385 g. The lumen of the aorta in this size rat is in the range of 1–2 mm in diameter, which is representative of the most distal part of human coronary arteries that can be imaged at CCTA using contemporary CT scanners.

To simulate the thorax of an overweight-to-obese patient, we used a custom version of a commercial phantom (QRM-Thorax, QRM, Moehrendorf, Germany) that was enlarged to the diameter of a large thorax by encasement within an “extension ring” (QRM, Moehrendorf, Germany) made of tissue-equivalent plastic. Our phantom is 200 mm in the longitudinal dimension, rather than the standard 100 mm. The outside dimension of the phantom with extension ring is 300 mm in the anterior-posterior (AP) direction and 400 mm in the lateral (LAT) direction. The thorax phantom includes a 100 mm diameter cylindrical hole in the mediastinum region to accommodate a myocardial insert. In this hole, we inserted an anesthetized rat on a bed locally fabricated from polymethyl methacrylate (PMMA) tubing with 3.5 mm thick walls. We gently placed tissue-equivalent plastic rods (CIRS, Norfolk, VA, USA) around the rat.

Injection Protocol—Prior to placing the rat in the phantom, we anesthetized the rat using 3% isoflurane in oxygen in an induction chamber at 1.5 L/m. The rat was weighed. We placed the rat on the PMMA bed and maintained isoflurane anesthesia at 1.5 L/m through a nosecone. We then inserted a 26 gauge catheter in the rat’s tail vein, and placed plastic rods on the bed with the rat. The bed, with rat and rods, was inserted into the phantom.

With a goal to reduce inter-animal variability of the vascular contrast enhancement, and therefore improve the validity of the averaged enhancement curves, we used animal-weight-normalized injection parameters. According to each rat’s weight, we determined the volume of contrast agent to be injected, and therefore the injected dose (see Table 2). We chose the injected volume to produce an injected dose of 529 mg active element/kg bodyweight, corresponding to a clinically-relevant dose of 100 mL of 370 mg/mL contrast agent in a 70 kg patient. With the goal to produce the same bolus width in each animal, we calculated injection rates required to produce a total injection time of 6 s, given the volume to be injected into that animal. From our experience, we anticipated achieving a clinically-relevant

concentration in the rat's aorta of approximately 10 mg/mL, using this injection protocol strategy.

After we placed the rat in the phantom, we connected the catheter to a 5 mL Luer Lock syringe that was installed in a model NE-1000 syringe pump (New Era Pump Systems, Farmingdale, NY, USA). Before connecting, we primed the 0.5 mm diameter tubing (Minibore Extension Set 36, Hospira, Lake Forest, IL) connecting the syringe to the catheter with contrast agent. Simultaneously with the start of scanning, we initiated the pre-determined injection of contrast agent into the rat's tail vein.

CT Scanning Protocol—We did not mechanically ventilate the rat, and a rat's heartbeat is far too high to be able to perform cardiac-gated CT scans on a clinical CT scanner. Therefore, imaging the abdominal-thoracic aorta and vena cava is quite challenging because the images of these vessels are subject to blurring due to cardiac and respiratory motion. There can be a substantial difference in the apparent image contrast enhancement of these vessels, depending on whether the image is acquired during inhalation/exhalation or during the respiratory resting phase. Our goal was to quantitatively compare the image contrast produced by the two contrast agents; if we did not use a rigorous method to control for the motion blurring, our results would be substantially affected. We therefore used a heavily-oversampled and retrospective time-point selection method, as described in the following paragraphs.

We used a 64-row CT scanner (LightSpeed™ VCT; GE Healthcare, Little Chalfont, United Kingdom) with 140 kVp; 300 mA; 40-mm collimation; large bowtie filter; 0.4-second rotation. A tube current of 300 mA was chosen, as this is the upper limit for the small focal spot. The small focal spot was desired to ensure resolution of the rats' great vessels. We first performed unenhanced axial scans in order to locate an ideal longitudinal position in the rat's thorax to image the vena cava and aorta; we used the last rib as a reference. At that position, the aorta is far enough from the spine to be able to distinguish it, and both vessels are into the liver and therefore the effect of respiratory motion is minimized. We started the scan protocol and simultaneously initiated the injection; this resulted in the beginning of enhancement in the abdominal vena cava approximately 1 second after the start of scanning. For 16 seconds, we scanned the rat's thorax at the pre-selected position in "cine" mode – continuous axial acquisitions. We reconstructed these projection data at 50 ms intervals; therefore, we obtained reconstructed volumes of the rat's thorax at a frequency of 20 volumes/s (2.5 volumes / gantry rotation). This permitted us to retrospectively select volumes where the visible contrast enhancement in the vena cava and aorta was at a local maximum, and therefore image blurring from respiratory motion was presumably at a minimum. We performed these reconstructions using the "standard" kernel; 512 × 512 pixel axial images; a 16-cm field of view (FOV) resulting in 0.3125 pixels in the axial images; and 64 0.625 mm-thick images per image volume (time point).

Following the 16-second cine scan of the rat's thorax, we scanned the entire rat in helical mode, using the same scan parameters as the cine scan, and a pitch of 0.984. For the first few minutes we scanned every 7 seconds, and then progressively increased the inter-scan delay as we continued scanning for one hour. We reconstructed images using the same

parameters as the cine scans, except that we reconstructed 321 0.625 mm-thick images per image volume (time point), covering the entire 200 mm length of the phantom, and including the entire rat.

Vessel Segmentation and quantification of contrast enhancement—A detailed description of the process used to segment the rats' vessels and quantify the contrast enhancement is available as Text in Supplemental Digital Content 2. Summarizing, we first segmented the vessels at each time point, using proprietary motion-tracking software developed using Matlab (MathWorks, Natick, MA). Then, using digital signal processing techniques, we selected the time points during which there was minimal motion, resulting in an attenuation-versus-time curve for each of the rats' aorta and vena cava. Finally, we normalized each curve in time such that they were synchronized at the rising edge of the bolus in the vena cava; we subtracted the un-enhanced attenuation of blood (60 HU) from each curve; and we averaged curves for each vessel imaged with the same contrast agent. This resulted in curves showing contrast enhancement versus time, for each vessel and contrast agent.

Biological Studies

Contrast agent preparation—For *in vivo* safety studies, we prepared the agent in an identical manner to methods previously published.¹² Briefly, CZ-TaO NPs were concentrated to 150 mg Ta/mL, and then formulated to iso-osmolality using 10X concentrated phosphate-buffered saline (PBS). To determine sterility before *in vivo* studies, we used two different techniques for detecting endotoxin. In the first method, we measured the amount of endotoxin present in the agent using an EndoSafe®-PTS™ (Charles River Laboratories, Wilmington, MA). For the second method, TaO NPs were tested for bacterial or endotoxin contamination using the standard limulus amoebocyte lysate (LAL) chromogenic assay. It has been reported in previous studies that nanomaterials can interfere with this assay.^{22,23} Thus, materials that were qualified to be less than 0.3 EU endotoxin/gram of tantalum were advanced to *in vivo* studies.

Acute Tolerability and Tissue Retention—We performed studies of acute tolerability and tissue retention in an identical manner to methods previously published.¹² We used naïve Lewis rats (Charles River Laboratories, Wilmington, MA) to determine the tolerability of this agent in a healthy animal (n = 2 to 4 per study). These studies included injecting the agent at the nominal anticipated clinical dose (ACD) of 400 mg Ta/kg, and at 3 times and 6 times higher than the high end of the range of ACD (1500 mg Ta/kg and 3000 mg Ta/kg, respectively), followed by longitudinal hematology (from 4 hours to 1 week) to assess impact to blood cells and organ function, and histological analysis of kidneys at 48 hours. Rats were anesthetized using isoflurane when injecting CZ-TaO NP and saline, and when drawing blood. We used a Hemavet 950 (Drew Scientific, Oxford, CT) for complete blood count (CBC) measurements. Tissues were stained with hematoxylin and eosin (H&E), analyzed by a toxicologic histopathologist, and scored as outlined in Table 3.

We measured tantalum retention in several organs (liver, kidney, spleen, heart, lung, brain, stomach, intestines) and in the whole carcass 48 hours after injection at ACD. Target

clearance organs such as the liver, kidney and spleen were the focus of previous studies, but in this evaluation we used identical methods¹² to explore the entire carcass of the rats for evidence of significant retention in any other organ.

An additional study was performed to evaluate blood clearance rates of CZ-TaO NPs after injection. CZ-TaO NPs were injected at 300 mg Ta/kg and blood was collected via tail or saphenous vein in rats (n = 5) at various time points (pre-injection, 5, 15, 30 minutes, 1, 3, and 6 hours). Tantalum in blood was measured by ICP-OES using methods described in previous work.¹²

Acute Kidney Injury: MSD Assay—We injected male Lewis rats (n = 4) intravenously with 3 times the high end of the range of ACD (1500 mg Ta/kg) of either CZ-TaO NPs or iopromide. We used gentamicin (APP Pharmaceuticals, Schaumburg, IL, product No. 63323001020) as a positive control, using a reported concentration and dosing schedule confirmed to cause kidney injury.²⁴ We conducted a metabolic study, collecting urine at 4, 24, 48 hours, and 7 days after injection. We used a kidney injury panel 1 assay (cat. No. K15162C, Meso Scale Diagnostics, Rockville, MD) to detect kidney biomarkers of kidney injury: neutrophil gelatinase-associated lipocalin (NGAL or lipocalin-2), albumin, and T-cell immunoglobulin and mucin domain 1 (TIM-1), also known as kidney injury molecule-1 (KIM-1). We diluted urine samples ten-fold prior to running the assay. We reported data as concentration (ng/mL) of each biomarker. We used a Student's T-test to determine statistical significance.

CZ-TaO NP contrast agent chemistry

Preparation—We obtained tantalum ethoxide (Ta(OEt)₅) from H. C. Starck (Munich, Germany) and used as received. We prepared deionized water (18.2 MΩ cm resistivity) with a Milli-Q® Biocel (Millipore SAS, Molsheim, France) filtration system, equipped with a Quantum® EX Ultrapure Organex (Merck KGaA, Darmstadt, Germany) cartridge and 0.22 μm filter. The silane, (*N,N*-dimethylaminopropyl)trimethoxysilane, product code SID3547.0 (Gelest, Inc., Morrisville, PA) was purified by distillation. We used SnakeSkin® (Thermo Fisher Scientific, Waltham, MA) regenerated cellulose dialysis tubing. All other reagents and solvents were purchased from Sigma Aldrich or Fisher (Thermo Fisher Scientific, Waltham, MA) and used as received. Details of the synthesis of CZ-TaO NPs can be found as text in Supplemental Digital Content 3.

Physicochemical Analysis—We analyzed CZ-TaO NPs using a number of methods. We measured hydrodynamic size of the particles by dynamic light scattering (DLS) at 25°C using a ZetaPALS analyzer (Brookhaven Instruments Corporation, Holtsville, NY). The mean diameter was measured based on the $Z_{\text{effective}}$ of volume-weighted-based distribution. We used multi-dimensional nuclear magnetic resonance (NMR) to determine the surface functionality of these nanoparticles. We measured spectra on a Varian (Varian Inc., formerly Palo Alto, CA) 600-MHz instrument NMR spectrometer. We measured osmolality and viscosity of the agent at a wide range of tantalum concentrations, including at high concentrations required for bolus injection in standard clinical CT imaging practice. We measured viscosity using an Anton Paar (Graz, Austria) AMVn capillary viscometer to

determine the dynamic and kinematic viscosity of aqueous solutions at 37°C, and we measured osmolality using a Wescor Vapro (ELITech Group, Puteaux, France) model 5520 osmometer in an identical manner to methods previously published.¹² We performed elemental analysis in a manner identical to methods previously published¹² using inductively coupled plasma optical emission spectroscopy (ICP-OES) quantification (Spectro Arcos, Kleve Germany), which enabled us to determine percent Ta and percent Si (by weight) in the product and percent yield of product based on the mass of Ta used as starting material, absolute concentration of nanoparticle solutions, and the amount of material retained in tissues after *in vivo* studies.

Results

Imaging Studies

The measured mass concentrations of the injected contrast agents, nominally 138 mg element/mL, were 142 mg iodine/mL and 139 mg tantalum /mL (Table 1).

The weights of the rats that were used, and the associated contrast agent injection parameters, are shown in Table 2. The rats' average weight was 366 g, and the largest and smallest were +5% and -7% of the mean. The injected dose of the active element for each scan was in the range of 180 mg to 204 mg; injection rates ranged from 0.217 mL/s to 0.246 mL/s.

A representative CT image of a rat within the entire assembled phantom is shown in Figure 3. In this image, we chose the display window and level so that the contrast-enhanced cross-sections of the rat's vena cava and aorta can be clearly seen; these vessels successfully represent the coronary arteries in a human patient.

The contrast enhancement in the rats' vena cava and aorta was successfully estimated for each rat, using the method described. A typical raw segmentation process is shown as a movie in Supplemental Digital Content 4. Representative images from the vessel segmentation process, taken from the time of peak enhancement in each rat's aorta, are shown in Figure 4. The vena cava and aorta are labeled in each image. These images are displayed at WW=600, WL=300, so that the difference in conspicuity of the iodine-enhanced aorta and the tantalum-enhanced aorta is clearly apparent. The temporal filtering process is depicted in Figure 5-1, Supplemental Digital Content 5. An example of temporal registration, and averaging the attenuation from curves from multiple rats, is shown in Figure 5-2, Supplemental Digital Content 5. The bolus width at 400 HU is approximately 5 ± 1 s. Figure 5 shows the averaged results for the measured contrast enhancement. The peak value for iodine in the vena cava was 851 HU (s.d. 34 HU); the peak value for tantalum was 1270 HU (s.d. 79 HU), for a 49% improvement using tantalum. The peak values in the aorta were 211 HU (s.d. 15 HU) and 295 HU (s.d. 4 HU) for iodine and tantalum respectively, for a 40% improvement using tantalum. The curves from each rat were registered temporally at the rising edge of the vena cava enhancement, resulting in small error bars at early times in the vena cava curves. Inter-animal variability causes the error bars to be larger at later times in this curve. The aorta curves for each animal were adjusted in time the same as the vena cava curves; intra-animal variability thus causes the entire aorta curves to have similar error

bars. Note that only two rats injected with CZ-TaO NP-based contrast agent were scanned; therefore, the error bars for the averaged enhancement with tantalum are larger than those for the iodinated agent.

Representative images of two rats' abdomens during a few of the later time points are shown in Figure 6. Qualitatively, at each time point iopromide and CZ-TaO NPs produce generally similar contrast enhancement in the organ parenchyma, specifically the liver, kidney cortex, and kidney medulla. To varying degrees, the CZ-TaO NPs produce brighter features, which can be at least partially explained by the higher contrast enhancement that tantalum provides compared with iodine. It seems that kidney enhancement may be earlier and much brighter with CZ-TaO NPs, such as seen at the 22 minute time point.

Biological Studies

Acute Tolerability and Tissue Retention—Tissue retention results are presented in Figure 7. At ACD, the percent ID retained (mean \pm s.d.) was 0.08 ± 0.01 in liver, 0.38 ± 0.08 in kidneys, 0.29 ± 0.22 in gastrointestinal (GI) tract; these were less than the retention found in the same organs of a clinically-used iodine-based contrast agent: 0.20 ± 0.08 in liver, 0.50 ± 0.05 in kidneys, and 0.4 ± 0.06 in GI tract.²⁰ In addition, histopathological examination of tissues taken from the injected animals at ACD and at 3 times ACD after 48 hours showed no evidence of damage to kidney (Table 3), in agreement with our previous rat studies with zwitterionic TaO NPs.¹³ Results from kidney analysis provide evidence that these materials are cleared from the kidney with no observable pathology.

Longitudinal hematology data of animals injected at ACD, 3, and 6 times higher than ACD (from 4 hours out to 1 week), including the normal range as provided by the manufacturer of the CBC measurement system, can be found in Tables in Supplemental Digital Content 6 and Figures in Supplemental Digital Content 7. These data (complete blood count (CBC) and clinical chemistry) did not show statistically significant effects from injection of CZ-TaO NPs when compared with the saline-injected control and with the naïve (pre-injection) rats in the same group.

We converted the measured tantalum concentration in the blood to percent ID (see Figure 8-1, Supplemental Digital Content 8). This revealed that at 5 minutes, 9% of the ID remained in the blood. We modeled elimination-phase pharmacokinetics (PK) and applied a bi-exponential fit to the results. This identified a dominant elimination half-life of 14 minutes that accounted for 97% of the tantalum, and secondary half-life of 158 minutes that was associated with the remainder (see Figure 8-2, Supplemental Digital Content 8).

Acute Kidney Injury: MSD Assay—See Figures, Supplemental Digital Content 9. Urine tests for acute kidney injury markers albumin and TIM-1 showed no differences from saline control or iopromide at four time points (4, 24, 48 hours, 1 week) following injection of CZ-TaO NPs at 3 times the ACD. Compared to previously reported PHS-TaO, where histopathology indicated damage to kidney cortex,^{11,12} lower albeit detectable responses in NGAL were measured at 24 and 48 hours; these returned to a response indistinguishable from either saline control or iopromide by 1 week.

Chemical characterization

We confirmed the structure of the CZ-TaO NP coating with NMR spectroscopic data. The ^1H NMR spectrum of CZ-TaO NPs with peak assignments is shown in Figure 8A. These assignments were confirmed by two-dimensional (2D) NMR spectroscopy as shown in Figure 8B. The peak assignments indicated in Figure 8B were used to rationalize the correlations observed in the 2D spectrum. Results clearly identify carboxybetaine functionalized particles, but also the presence of residual isopropyl ester in the final product. By integration, the final zwitterionic product contains about 8.5% of residual isopropyl ester. In addition, a ^{13}C spectrum of CZ-TaO NPs was obtained to complement the ^1H NMR data (see Text, Supplemental Digital Content 3). Furthermore, a heteronuclear multiple-bond correlation (HMBC) 2D experiment was performed to show a connection between ^1H peak **a** (Figure 8A) and ^{13}C carbonyl **B** (Figure 8B) through peak **Ba**. The 162–175 ppm region of the ^{13}C spectrum is included in Figure 8B from the HMBC experiment.

The average particle size $Z_{\text{effective}}$ (by volume) was determined by DLS to be 3.1 nm for a 25 gram scale reaction, and this was typical. Nanoparticle size distribution was narrow (i.e. s.d. approximately 0.5 nm) and standardized by a purification process that involved molecular weight cutoff filters without detriment to reaction yield. Also typical was the weight percent of tantalum in the product (33.5%) and the Si:Ta mole ratio (1.49) as measured by ICP-OES. The yield of the reaction following purification by dialysis was 58.3% based on tantalum content, and the silicon utilization was 43.5%.

The viscosity and osmolality of aqueous solutions of CZ-TaO NPs were measured as a function of tantalum concentration and are reported in Figure 9.

While sterility of CZ-TaO NPs was achieved by sterile-filtration, nanoparticles were stable to autoclave conditions. A 25 mg Ta/mL solution of CZ-TaO NPs in D_2O was autoclaved in a 45 minute cycle including 15 minutes at 100 °C. The average particle size by DLS, $Z_{\text{effective}}$, was unchanged, being measured as 3.03 nm before autoclaving and 3.05 nm after the cycle. Nanoparticles remained size-stable (as monitored by DLS) and well-dispersed in aqueous solution after autoclave conditions. The ^1H NMR spectrum recorded 5 days later was indistinguishable from that recorded before autoclaving, except for indicating a small amount of isopropyl ester hydrolysis (see Figure 8A).

Discussion

Imaging Studies

Dynamic vessel enhancement measurements—The method we used, an extension of a method reported earlier,²⁵ enabled us to quantify CT attenuation in the great vessels of a free-breathing rat. Using this method, we were able to gain insight into the dynamic performance of the CZ-TaO NP-based agent in comparison to an iodinated agent.

Published results for CT contrast enhancement improvement using tantalum compared with iodine at 140 kVp are in the range of 50–65%.^{16,17} However, these results were obtained using large, dense phantoms that represent the abdomen of an overweight-to-obese adult. The effect of these phantoms is to “harden” the X-ray spectrum, increasing the mean energy

of the spectrum. The imaging benefit of tantalum-based contrast agents increases with the size and density of the subject being scanned, such as would be seen with obese adults. The reason for this is that the X-ray attenuation produced by tantalum does not diminish as substantially as with iodine when imaged with higher X-ray spectra.^{11,16,17} The 40–49% improvement in contrast enhancement that we observed in tantalum over iodine contrast in our large thorax CCTA model supports the hypothesis that tantalum contrast material should provide a substantial benefit for CT angiograms, especially CCTA for obese patients.

In the vena curves of Figure 5, we observe that the CZ-TaO NP bolus is wider and delayed with respect to the bolus from the iodinated agent. We hypothesize that the slightly higher viscosity of CZ-TaO NP (15–20 % higher viscosity than iopromide at 150 mg/mL; see Figure 9) leads to slightly slower dilution in the blood, thus higher concentration in the vena cava – at this point the blood has flowed only a few centimeters, and it flows slightly slower, leading to the broader/delayed bolus.

Reviewing the Figure 5 curves for the aorta, we note that the bolus of the CZ-TaO NP agent is quite similar in shape to that of the iodinated agent, and the CZ-TaO NP bolus is delayed with respect to the bolus of iodinated agent by approximately the same time as was found in the vena cava. This suggests that although there is a very slight difference in venous pharmacokinetics between the two agents initially, there was little subsequent effect on arterial pharmacokinetics. Accounting for the initial delay in venous arrival, the two agents then appear to have moved through the right heart, the pulmonary circuit, and the left heart almost identically. The CZ-TaO NPs, approximately 3 nm in diameter and twice the size of iopromide molecules (see Figures in Supplemental Digital Content 1), appear to move through the heart and capillaries in the lungs with comparable speed as the small molecule iodinated agent.

Weight-based injection protocol—Given the variation in rat weight of approximately $\pm 6\%$ of the mean, we intuitively anticipated that the enhancement might be approximately 6% above average in the smallest animal and conversely, if injected dose and injection rate were held constant for all animals (i.e., if no adjustment were made for weight). Because we held the injection time constant, we expected the bolus width to be fairly consistent. Because we adjusted the dose and rate based on animal weight, we had hoped to reduce the anticipated variability in enhancement. Reviewing Figure 5-2 in Supplemental Digital Content 5, which includes four scans with iodine (two using the same animal), we found that the variability in bolus width was approximately $\pm 20\%$. Since the injection time was held constant at 6 seconds, we attribute the $\pm 20\%$ variability to inter-animal variability. This suggests that if no adjustment had been made for weight, the variability in enhancement might have been even higher than $\pm 20\%$, due to the $\pm 6\%$ variability in animal weights. However, with our weight-normalized protocol we observed approximately $\pm 5\%$ variability in enhancement. Based on only one group of four animals, we are very cautious about drawing a firm conclusion; however, it appears that our protocol may have served to minimize inter-individual variation in our results.

Biological Studies

CZ-TaO NPs have, by far, the lowest retention of tantalum of any TaO NP that has been reported to date. CZ-TaO NPs cleared efficiently from the blood of injected animals with no observable effects to blood chemistry, organ function, or kidney pathology. Longitudinal hematology data showed no significant impact to blood cells or organ performance. Evaluation of blood clearance rates for CZ-TaO NPs, although determined at relatively high dose (300 mg Ta/kg), showed an elimination half-life that is shorter than iodixanol injected at a lower dose.²⁰

Iodixanol has a known retention profile when studied at ACD in normal rats.²⁰ The fraction of the clinically-required ID that is retained in the entire animal is quite low, with the highest level of approximately 0.5% ID observed in the kidneys. Many nanomaterials tested under similar conditions demonstrate significant retention in spleen and liver.²⁶ Zwitterionic shells have a major impact on clearance, though not all zwitterionic shells can impart the same levels of efficient clearance. Of the few tantalum-based agents about which biological data have been reported, CZ-TaO is, by far, most efficiently cleared from blood and from the organs of animals.^{13,27} The 48-hour retention measured for CZ-TaO NPs injected at 400 mg Ta/kg was very similar to the 24-hour clearance of iodixanol injected at 300 mg I/kg.²⁰ Based on the very low retention of CZ-TaO NPs in both liver and spleen, CZ-TaO NPs do not appear to have an affinity for the reticuloendothelial system or lymph node macrophage.

The absolute WBC results fell within the normal range. In most cases, the differential WBC results fall outside the normal range; however, many deviations from the normal range were not statistically significant. Furthermore, when compared with the saline control, the change in each group of rats versus the naïve (pre-injection) values tended to follow the same trend, within the statistical limits of our study (see Tables in Supplemental Digital Content 6 and Figures in Supplemental Digital Content 7). Therefore, we detected no significant impact to blood cells or organ function as a result of high doses of CZ-TaO.

Our blood concentration experiment was intended to elucidate the elimination kinetics of the CZ-TaO NPs. At the first time point that we measured (5 minutes), the blood contained only 9% of the ID, indicating a fast distribution phase into interstitial space. This is as we expected and is consistent with the 3 nm size of CZ-TaO NPs. Plotting the elimination-phase data on a semi-log plot (see Figure 8-2, Supplemental Digital Content 8), it is clear that there are two very distinct clearance mechanisms involved. The faster process has a half-life of 14 minutes, and dominates elimination during the first hour. This clearance mechanism accounts for approximately 97% of the tantalum (from the ratio of the exponentials at $t=0$, $8.8e^0/(8.8e^0+0.3e^0)$). The slower process, with a half-life of 158 minutes, is associated with only 3% of the tantalum.

These results give rise to the question: what is the root-cause explanation for the bi-phasic clearance that we observed? One hypothesis relates to nanoparticle size distribution, and the relationship of those sizes to capillary endothelial permeability. The average CZ-TaO NP size is 3.1 nm, with a narrow distribution due to purification-fractionation. As we summarized in the Introduction, capillary endothelium is readily permeable to particles of this size. It has also been reported that there is a rapid decrease in permeability rate when

molecule size exceeds 3.6 nm.¹⁸ The faster clearance process that we observed is consistent with sizes smaller than 3.6 nm, which includes the majority of CZ-TaO NPs; small-molecule iodinated agents with a half-life of 25 minutes²⁰ are also smaller than the 3.6 nm size threshold. The slower clearance process that we observed with CZ-TaO NPs could be due to a small fraction of nanoparticles in the distribution that are slightly larger than 3.6 nm. The PK results and our hypothesis to explain them are consistent with our imaging results of the liver and kidney at later time points. Further studies will be required to evaluate our hypothesis and provide more detailed PK information. Studies should be performed using a larger number of animals and measurements at time points less than 5 minutes. In any case, the elimination half-life that we calculated, combined with tissue retention results, CBC and clinical chemistry results, kidney histopathology results, and liver/kidney parenchymal contrast enhancement results provide evidence that CZ-TaO NPs are cleared effectively and efficiently with no observable pathology, and with similar pharmacokinetics compared with a small-molecule iodinated agent.

Sensitive urine markers for acute kidney injury (albumin, TIM-1, NGAL) were monitored from 4 hours to 1 week after injection of CZ-TaO at 3 times the ACD. No differences were observed between CZ-TaO NPs and saline control or iopromide at any time point for albumin or TIM-1. Compared to previously reported PHS-TaO NPs, where histopathology indicated damage to the cortex of kidneys and observed degeneration-regeneration of tubular epithelium,^{11,12} a lower yet statistically significant response in the NGAL biomarker was observed at 24 hours. This fell by 50% after 48 hours, and by 1 week the level returned to that equivalent to the saline control and iopromide. Since NGAL is induced during inflammation and may indicate the progression of, or protection from, renal damage,²⁸ we note this response. However, we also note that this experiment was performed at 3 times the ACD and that histopathology analysis of kidneys following injection at the same dose after 48 hours did not reveal notable findings. In light of the NGAL response and despite the normal histopathology, we feel that further nephrotoxicity studies are required in order to understand this response.

Chemical synthesis and characterization of CZ-TaO NPs

In the preparation of CZ-TaO NPs, cores were synthesized by the controlled hydrolysis of tantalum ethoxide in the presence of isobutyric acid in an alcoholic solvent. We believe that the carboxylic acid functioned as a sacrificial coating ligand, loosely protecting the TaO cores until they were displaced in the final coating step. The acid-stabilized core particles were not isolated, but rather coated *in situ* upon the addition of the alkoxy silane solution and water. A complete synthesis (as a 25 gram scale reaction) and purification including sterile-filtration of CZ-TaO NPs is described in detail (see Text, Supplemental Digital Content 3).

In the ¹H NMR spectrum of Figure 8A, the sharp resonances associated with peaks c, d, e and h, represent the presence of free silane ligand which is not bound to the TaO core particle. This free ligand is in equilibrium with bound ligand which is a general feature of this class of particles at very low concentrations (0.5–30 mg Ta/mL), as has been described previously.¹³ The free ligand takes several days to reach equilibrium concentration and we

determined that it does not change under conditions of the autoclave experiment (at 25 mg Ta/mL) as described in the previous section. The spectra shown in Figure 8A and Figure 8B were generated from the same sample with a tantalum concentration of 23 mg Ta/mL, after reaching equilibrium. The concentration of free ligand decreases substantially as the particle concentration (mg Ta/mL) increases.

While results clearly identify carboxybetaine functionalized particles, residual isopropyl ester can be seen in the final product. This resulted from transesterification with the solvent and persisted through the relatively harsh hydrolysis conditions. By integration, the final zwitterionic product contains about 8.5% of residual isopropyl ester.

To maximize CT contrast in a clinical application, there is a drive to maximize concentration of the radiopaque element in a single sample dose. For TaO NPs, this is not limited only by the solubility of the particle, but also by the viscosity and osmolality of the nanoparticle formulation. Ideally, the osmolality of a pure particle solution prepared in water would have an osmolality near that of blood, or even more ideally, less than that of blood, to allow for the addition of excipients to the formulation. Nevertheless, mild hyperosmolality would still enable clinical translation because the majority of clinical intravenous iodinated contrast materials are hyperosmolar, and show osmolality approximately three times that of blood.

From the measurement of viscosity and osmolality (Figure 9), it can be seen that even at 250 mg Ta/mL, the viscosity of CZ-TaO is less than 12 mPa.s, which is the range of the viscosity reported for clinical dimeric agents such as iodixanol²⁹ and significantly lower than previously reported ZMS-TaO.¹³ The osmolality of CZ-TaO NP solutions remained significantly lower than that of blood (290 mOsm/kg), even up to 200 mg Ta/mL (Figure 9). Thus, the solution properties of CZ-TaO are reasonable for clinical applications in this concentration range.

Conclusion

Our study demonstrates the viability of zwitterionic TaO nanoparticles as an attractive platform for a general-purpose CT contrast agent. CZ-TaO NPs represent significant progress toward a low viscosity, iso-osmolar formulation appropriate for clinical use at CT. Biological performance in animals supports the conclusion that these compounds can compare favorably with the efficient renal clearance and excellent safety profiles reported for iodine-based contrast materials such as iodixanol.²⁰ Coupled with the improved imaging performance that have been demonstrated for tantalum nanoparticle-based contrast agents,^{11,12,16,17} CZ-TaO NPs represent a promising candidate for the next generation of clinical CT contrast agents.

Supplementary Material

Refer to Web version on PubMed Central for supplementary material.

Acknowledgments

Research reported in this publication was supported by the National Institute of Biomedical Imaging and Bioengineering of the National Institutes of Health under Award Number R01EB015476 (co-PIs: PJB, BMY). The

content is solely the responsibility of the authors and does not necessarily represent the official views of the National Institutes of Health. The authors would like to thank Janell Crowder for performing the elemental analysis characterization of particle compositions and treated tissue, Tracy Zhang and Thomas Early for 2D NMR spectroscopic analysis of CZ-TaO solutions, Dan Meyer for helpful PK discussions, and Eric McWhinnie for help constructing the phantom. PJB would like to dedicate his contribution to the memory of his father.

References

1. Davenport MS, Cohan RH, Khalatbari S, et al. The challenges in assessing contrast-induced nephropathy: where are we now. *AJR*. 2014; 202:784–789. [PubMed: 24660707]
2. Schopp JG, Iyer RS, Wang CL, et al. Allergic reactions to iodinated contrast media: premedication considerations for patients at risk. *Emerg. Radiol*. 2013; 20(4):299–306. [PubMed: 23430296]
3. Jost G, Pietsch H, Lengsfeld P, et al. The impact of the viscosity and osmolality of iodine contrast agents on renal elimination. *Invest. Radiol*. 2010; 45(5):255–261. [PubMed: 20375847]
4. Pugh ND. Haemodynamic and rheological effects of contrast media: the role of viscosity and osmolality. *Eur. Radiol*. 1996; 6(2):S13–S15. [PubMed: 8798050]
5. Seeliger E, Flemming B, Wronski T, et al. Viscosity of contrast media perturbs renal hemodynamics. *J. Am. Soc. Nephrol*. 2007; 18(11):2912–2920. [PubMed: 17942967]
6. Seeliger E, Lenhard DC, Persson PB. Contrast media viscosity versus osmolality in kidney injury: Lessons from Animal Studies. *BioMed Res. Int*. 2014; 2014:15.
7. Jakhmola A, Anton N, Vandamme TF. Inorganic nanoparticles based contrast agents for x-ray computed tomography. *Adv. Healthcare Mater*. 2012; 1(4):413–431.
8. Liu Y, Ai K, Lu L. Nanoparticulate x-ray computed tomography contrast agents: from design validation to in vivo applications. *Acc. Chem. Res*. 2012; 45(10):1817–1827. [PubMed: 22950890]
9. Lee N, Choi SH, Hyeon T. Nano-sized CT contrast agents. *Adv. Mater*. 2013; 25(19):2641–2660. [PubMed: 23553799]
10. Roessler A-C, Hupfer M, Kolditz D, et al. High atomic number contrast media offer potential for radiation dose reduction in contrast-enhanced computed tomography. *Invest. Radiol*. 2016 Epub ahead of print.
11. Bonitatibus PJ Jr, Torres AS, Goddard GD, et al. Synthesis, characterization, and computed tomography imaging of a tantalum oxide nanoparticle imaging agent. *Chem. Commun*. 2010; 46:8956.
12. Torres AS, Bonitatibus PJ Jr, Colborn RE, et al. Biological performance of a size-fractionated core-shell tantalum oxide nanoparticle x-ray contrast agent. *Invest. Radiol*. 2012; 47(10):578–587. [PubMed: 22836312]
13. Bonitatibus PJ Jr, Torres AS, Kandapallil B, et al. Preclinical assessment of a zwitterionic tantalum oxide nanoparticle x-ray contrast agent. *ACS Nano*. 2012; 6(8):6650–6658. [PubMed: 22768795]
14. Butts, MD.; Colborn, RE.; Bonitatibus, PJ., Jr, et al., inventors. Nanoparticle contrast agents for diagnostic imaging. US patent. 8,574,549. 2013 Nov 5.
15. Bonitatibus, PJ., Jr; Butts, MD.; Colborn, RE., et al., inventors. Nanoparticle contrast Agents for diagnostic imaging. US patent. 2010/027834A1, 2010/0278748, and 2010/0278749. 2010 Nov 4.
16. FitzGerald PF, Colborn RE, Edic PM, et al. CT image contrast of high-Z elements: phantom imaging studies and clinical implications. *Radiol*. 2016; 278(3):723–733.
17. FitzGerald PF, Lambert JW, Edic PM, et al. CT radiation dose at equal image contrast-to-noise ratio using iodine- and novel tantalum-based contrast agents: a large habitus phantom study. *RSNA*. 2015 PH277-SD-THA6.
18. Mehta D, Malik AB. Signaling mechanisms regulating endothelial permeability. *Physiol. Rev*. 2006; 86:279–367. [PubMed: 16371600]
19. Satchell SC, Braet F. Glomerular endothelial cell fenestrations: an integral component of the glomerular filtration barrier. *AJP-Renal*. 2009; 296(5):F947–F956.
20. Heglund IF, Michelet AA, Blazak WF, et al. Preclinical pharmacokinetics and general toxicology of iodixanol. *Acta Radiol. Suppl*. 1995; 399:69–82. [PubMed: 8610532]

21. Sovak M, Terry R, Abramjuk C, et al. Iosimenol, a low-viscosity nonionic dimer: preclinical physicochemistry, pharmacology, and pharmacokinetics. *Invest. Radiol.* 2004; 39(3):171–181. [PubMed: 15076009]
22. Dobrovolskaia MA, McNeil SE. Immunological properties of engineered nanomaterials. *Nat. Nanotechnol.* 2007; 2(8):469–478. [PubMed: 18654343]
23. Dobrovolskaia MA, Germolec DR, Weaver JL. Evaluation of nanoparticle immunotoxicity. *Nat. Nanotechnol.* 2009; 4(7):411–414. [PubMed: 19581891]
24. Ozer JS, Dieterle F, Troth S, et al. A panel of urinary biomarkers to monitor reversibility of renal injury and a serum marker with improved potential to assess renal function. *Nature Biotech.* 2010; 28:486–494.
25. FitzGerald PF, Torres AS, Bonitatebus PJ, et al. Contrast-enhanced functional imaging of rats using state-of-the-art clinical CT. *AMI & SMI.* 2007
26. Choi HS, Liu W, Misra P, et al. Renal clearance of quantum dots. *Nat. Biotechnol.* 2007; 25(10): 1165–1170. [PubMed: 17891134]
27. Oh MH, Lee N, Kim H, et al. Large-scale synthesis of bioinert tantalum oxide nanoparticles for x-ray computed tomography imaging and bimodal image-guided sentinel lymph node mapping. *J. Am. Chem. Soc.* 2011; 133(14):5508–5515. [PubMed: 21428437]
28. Mishra J, Ma Q, Prada A, et al. Identification of neutrophil gelatinase-associated lipocalin as a novel early urinary biomarker for ischemic renal injury. *J. Am. Soc. Nephrol.* 2003; 14(10):2534–2543. [PubMed: 14514731]
29. [Accessed November 30, 2014] Visipaque (Iodixanol) injection solution. NLM NIH. <http://dailymed.nlm.nih.gov/dailymed/archives/fdaDrugInfo.cfm?archiveid=4724>.

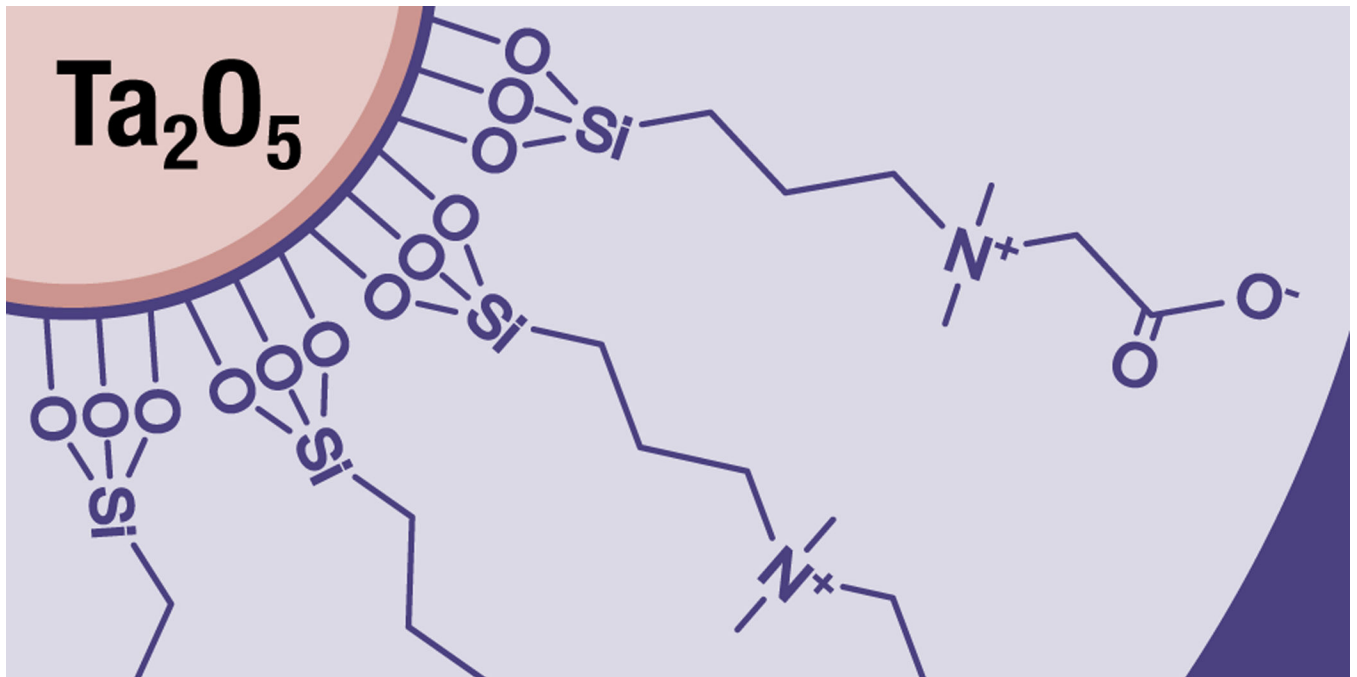


Figure 1.
Schematic diagram of carboxybetaine zwitterionic (CZ) coated soluble tantalum oxide nanoparticles (CZ-TaO NPs).

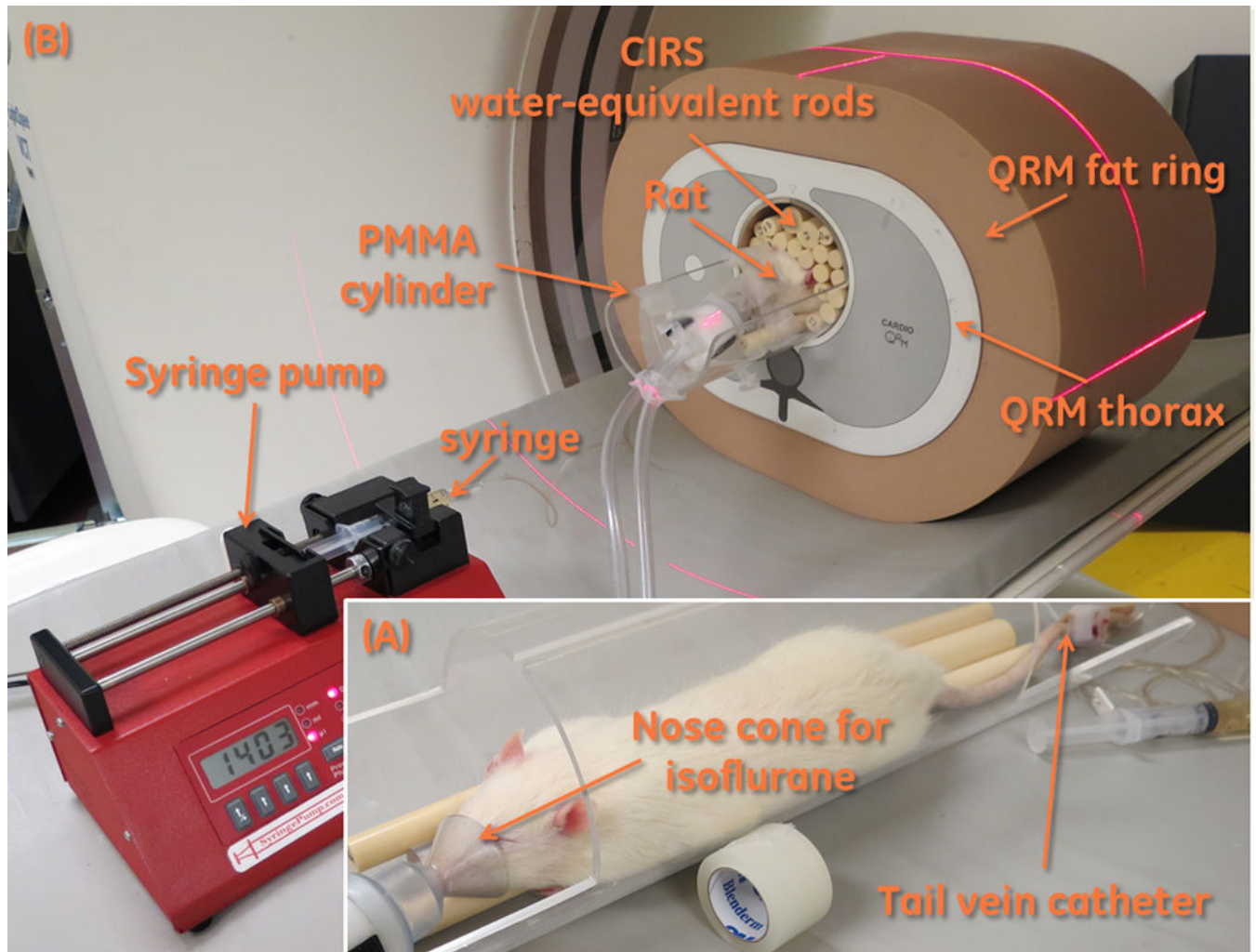


Figure 2.

(A) Positioning a rat for scanning. The rat has had a tail vein catheter inserted, and isoflurane anesthesia is being administered via a nose cone. The rat is placed on top of some water-equivalent plastic rods. (B) A complete assembled phantom. The anesthetized and catheterized rat is placed within the QRM phantom and fat ring. The syringe is connected to the tail vein catheter, and is installed into the syringe pump.

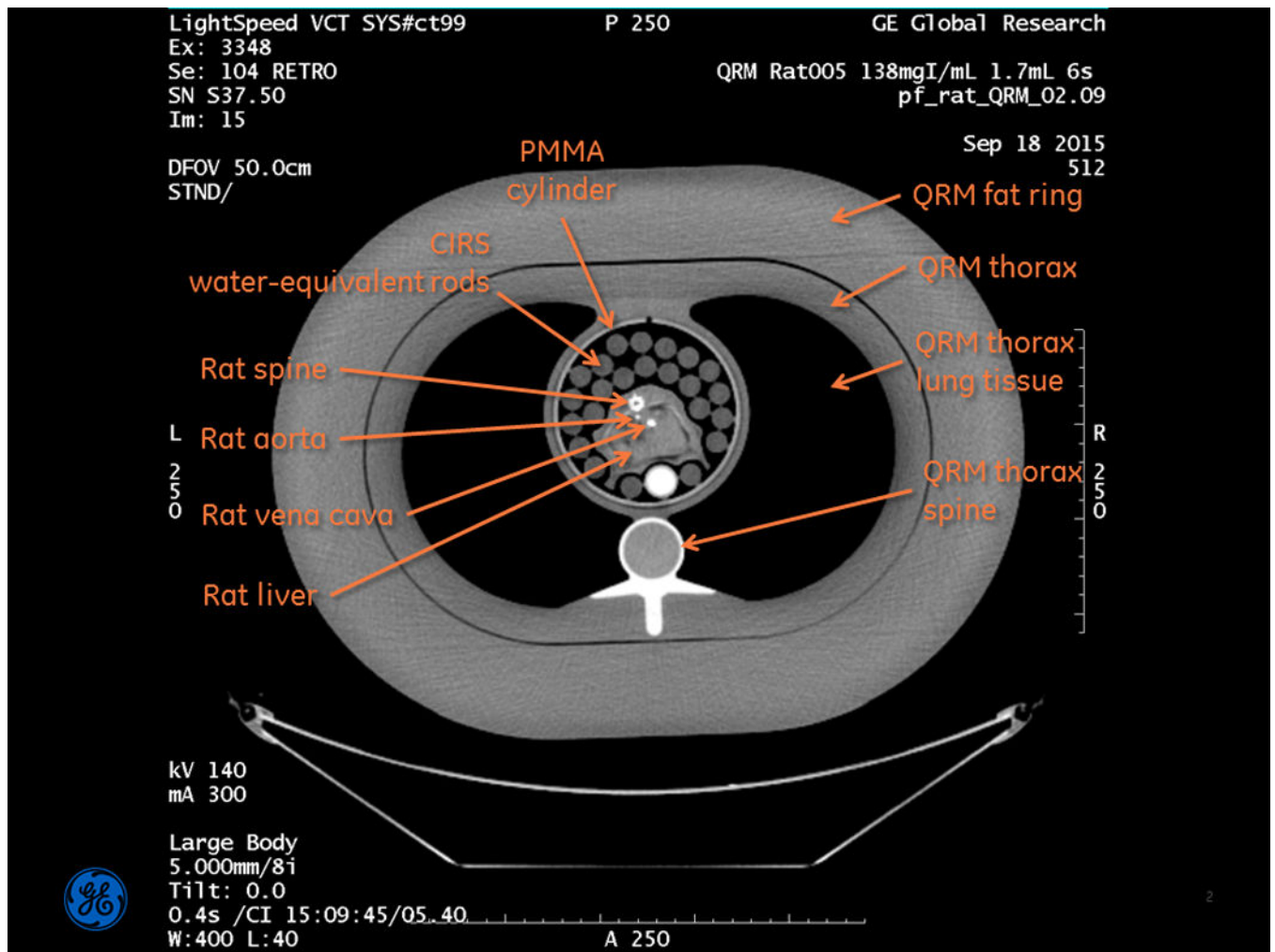


Figure 3.

Full field-of-view image of the assembled phantom. The contrast-enhanced cross-sections of the rat's vena cava and aorta can be seen, and represent the coronary arteries in a human patient. Note: this image was produced solely for reference purposes, and the reconstruction parameters are not what were used for subsequent quantitative analysis. This image is displayed at WW=400, WL=40, so that the vessels are clearly visible.

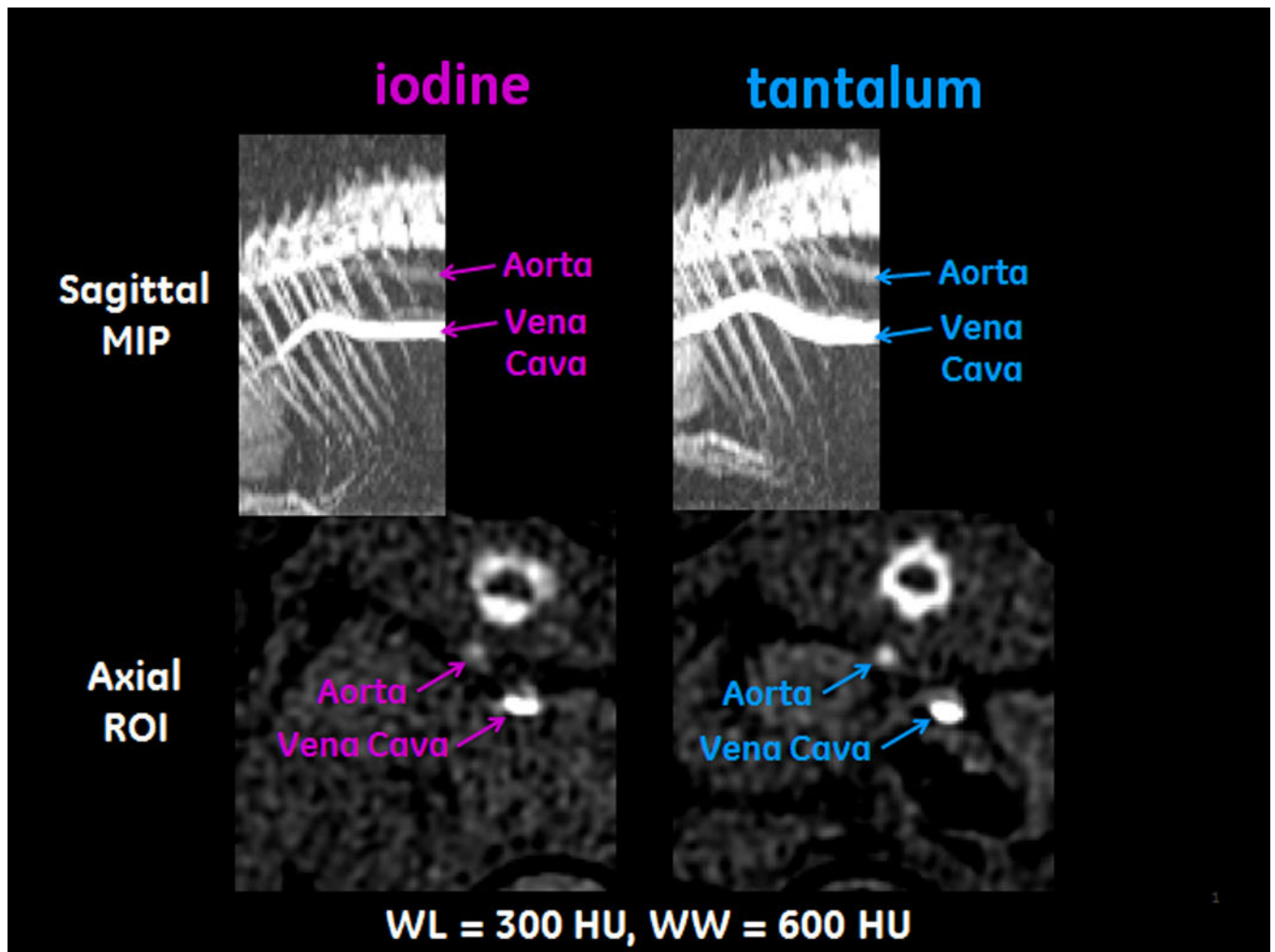


Figure 4. Images from the vessel segmentation process. These images are taken from the time of peak enhancement in each rat's aorta. The images on the left are of a rat injected with the iodinated agent; the images on the right are of a rat injected with CZ-TaO NP-based agent. The images in the top row are maximum intensity projections (MIPs) of the rats' thoraxes; the images in the bottom row are regions of interest (ROIs) taken from axial images corresponding to the rightmost column of pixels in the MIPs.

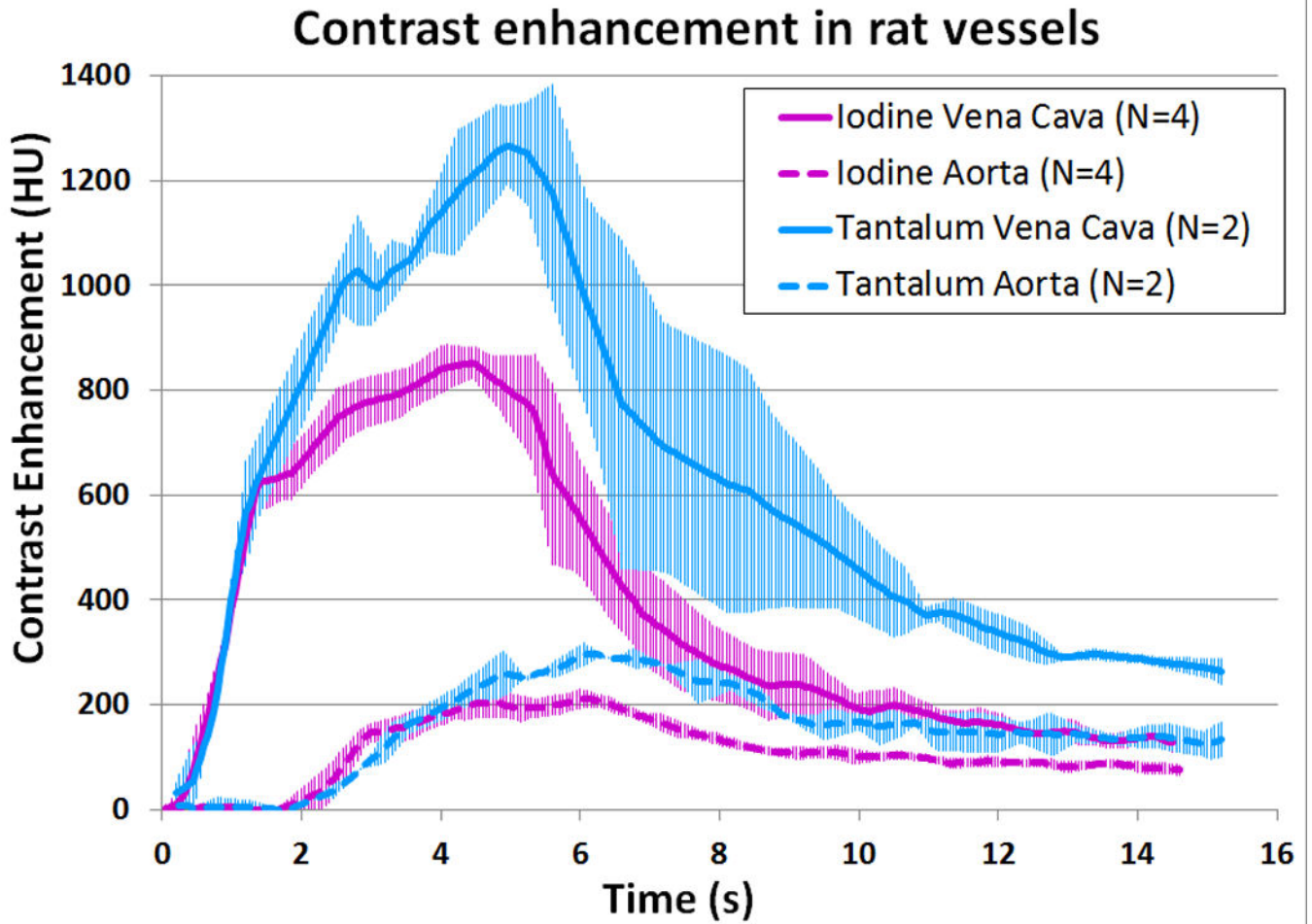


Figure 5.

Average contrast enhancement in the rats' vena cava and aorta. The error bars are ± 1 standard deviation (s.d.).

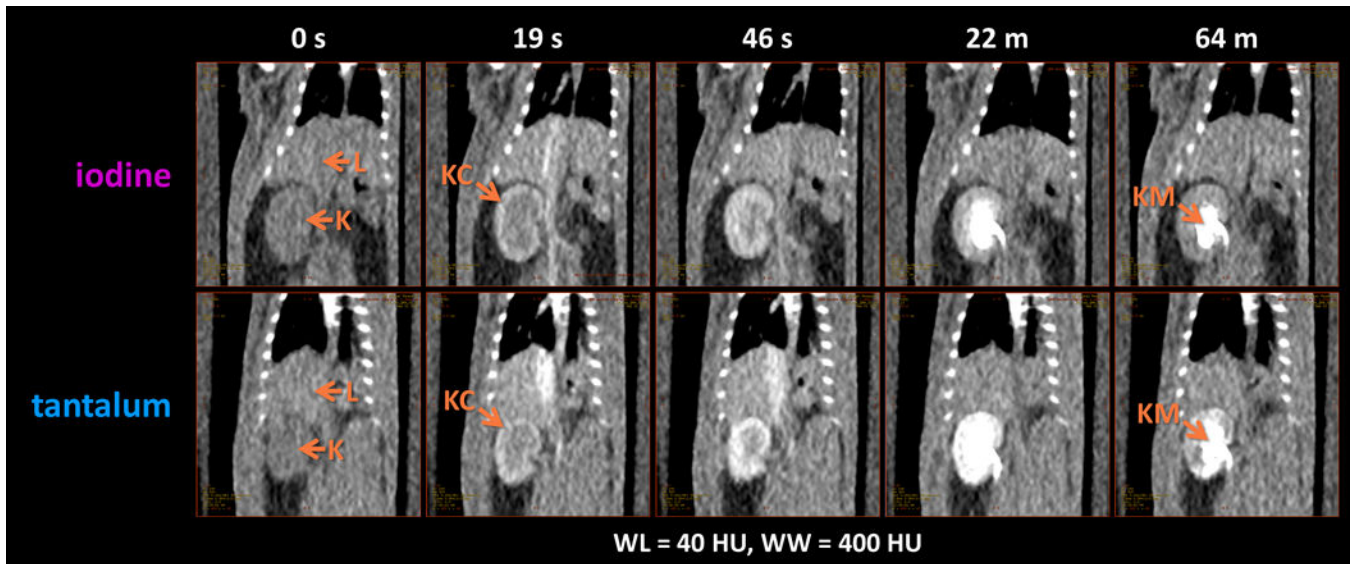


Figure 6. Typical CT images showing liver and kidney enhancement in normal rats, using iodine (iopromide) and tantalum (CZ-TaO NPs). Key: L=liver; K=kidney; KC=kidney cortex; KM= kidney medulla.

Tantalum retention in rats 48 hours after injection

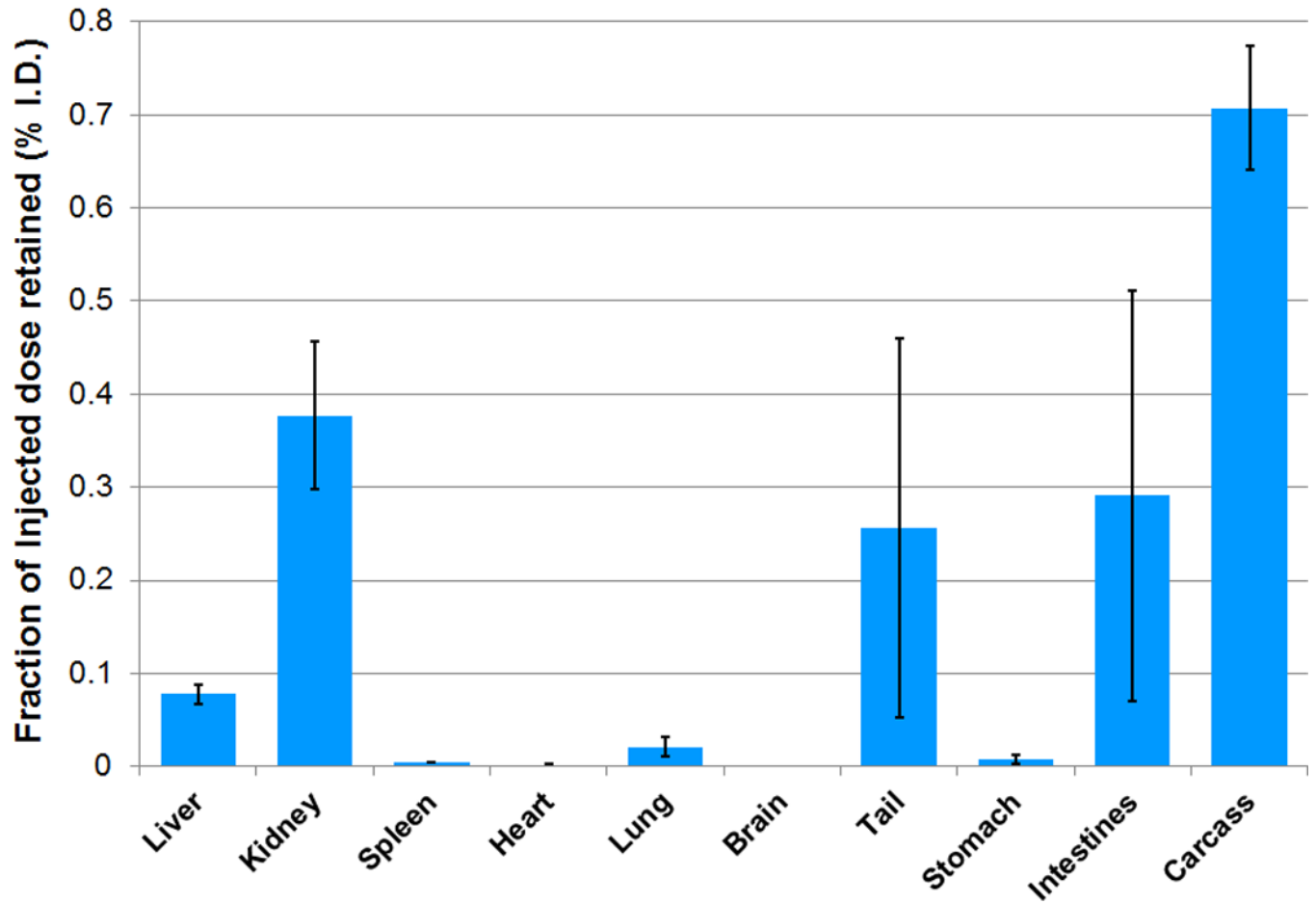


Figure 7.

Organ retention of CZ-TaO NPs in rats (n = 4) at a dose of 400 mg Ta/kg, after 48 hours.

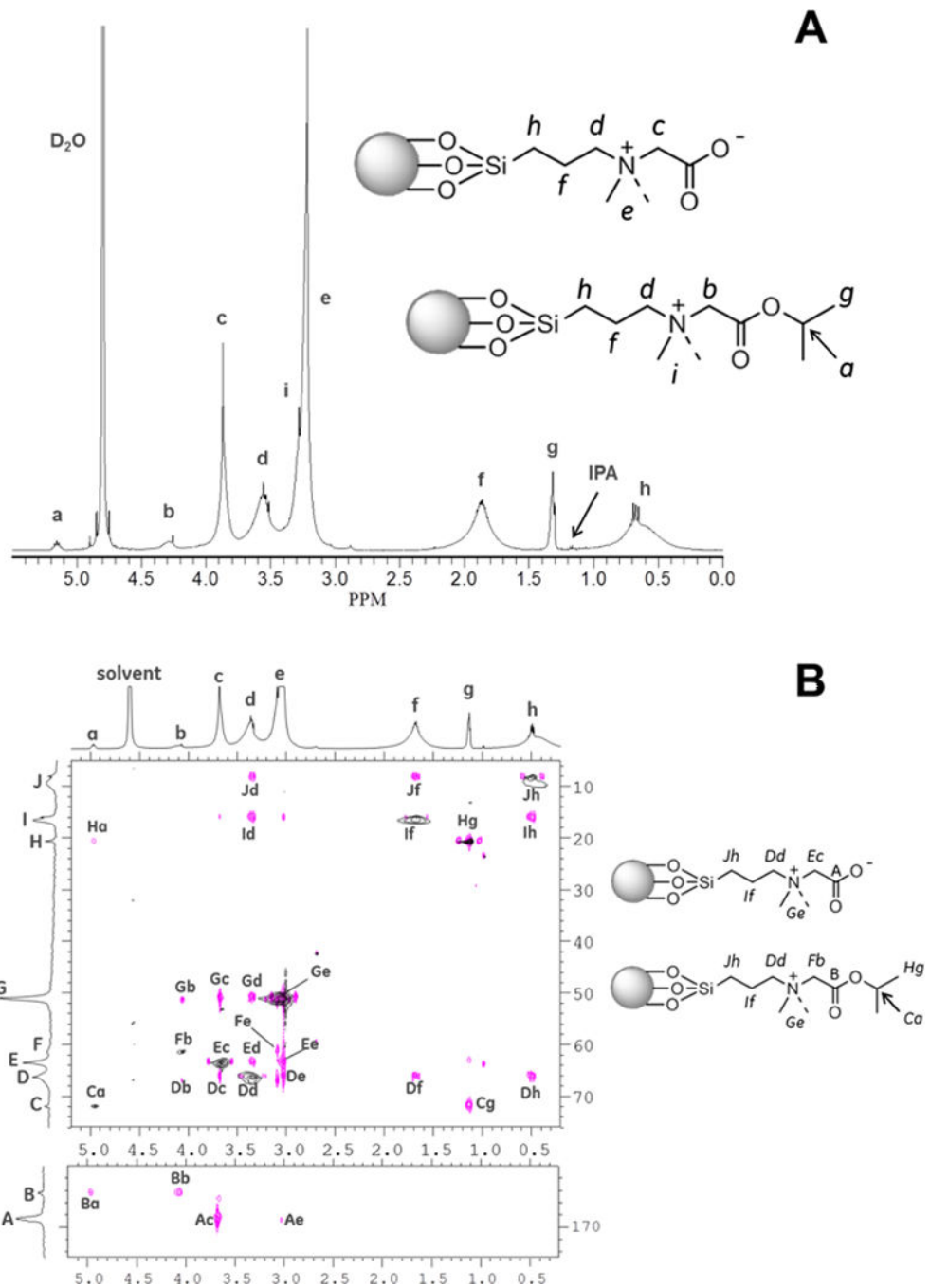


Figure 8. (A) Proton nuclear magnetic resonance (^1H NMR) spectrum of CZ-TaO NPs in D_2O . (B) Heteronuclear two-dimensional (2D) NMR spectra of CZ-TaO NPs in D_2O . Peak “Ba” establishes connection from ^1H peak “a” to ^{13}C carbonyl “B”.

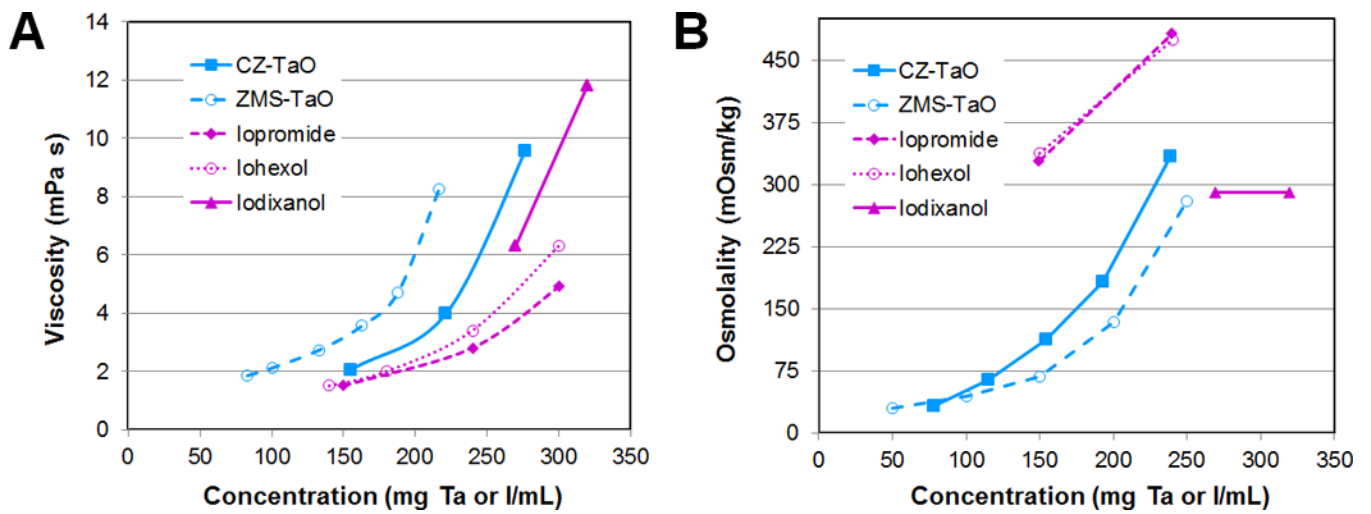


Figure 9.

(A) Viscosity and (B) osmolality of CZ-TaO NPs as a function of concentration compared to the previously reported ZMS-TaO¹³ and iodinated agents as formulated for injection by the manufactures.

Table 1

Contrast agent measurements

Parameter	Active element	
	Iodine	Tantalum
ICP-OES measurement (mg element/g)	122	114
Measured density (g element/mL)	1.16	1.22
Mass concentration (mg element/mL)	142	139

Author Manuscript

Author Manuscript

Author Manuscript

Author Manuscript

Table 2

Summary of rats scanned and injection parameters

Animal ID	Weight (g)	Contrast agent material	Injected volume (mL)	Injected dose (mg element)	Injection rate (mL/s)
Rat 7	386	Iopromide	1.48	204	0.246
Rat 4	357	Iopromide	1.37	189	0.228
Rat 7-2	375	Iopromide	1.44	198	0.240
Rat 6	340	Iopromide	1.30	180	0.217
Rat 8	366	CZ-TaO	1.40	194	0.234
Rat 10	372	CZ-TaO	1.43	197	0.238

Table 3
 Histopathology analysis of kidneys following injection of CZ-TaO at 1500 mg Ta/kg.

Kidney Pathology Feature	Saline			CZ-TaO		
	1	2	3	1	2	3
Tubular epithelium, cortex-Degeneration	N	N	N	N	N	1
Tubular epithelium, cortex-Regeneration	N	N	N	N	N	N
Tubule, cortex-Dilation	N	N	N	N	N	N
Cortex-infiltration, mononuclear cell	N	N	>1	N	N	N
Tubular epithelium, cortex-cytoplasmic droplets	N	N	N	N	N	N

Organs harvested 48 hours following injection. Grading scale: N=Normal; 1=Minimal; 2=Mild; 3=Moderate; 4=Marked; >=Multifocal